Electronic states of V-shaped semiconductor quantum wires in electric fields

Hong Sun*
Department of Physics, Shanghai Jiao Tong University, Shanghai 200030, People's Republic of China
and Department of Physics, The Chinese University of Hong Kong, Shatin, NT, Hong Kong, People's Republic of China
(Received 13 January 1998; revised manuscript received 7 April 1998)

The electronic states of the GaAs/$Al_xGa_{1-x}As$ V-shaped quantum wires (V-QWR's) in external electric fields are calculated. Large Stark shifts in the intersubband transition energies and sensitive variations in the intersubband transition strengths are predicated in the V-QWR's that we consider at moderate electric fields. [S0163-1829(98)03447-X]

In recent years, there has been a rapid development in microetching and epitaxial growth techniques aimed at the fabrication of high-quality one-dimensional semiconductor nanostructures. Among them, V-shaped semiconductor quantum wires (V-QWR's) (Refs. 1–3) have attracted considerable interest because of their easy tailoring of the electronic structures and potential applications in quantum-wire laser devices.[2] In order to predict the physical properties and enable a better understanding of the experimental results of the V-QWR's, a number of calculations have been carried out using the tight-binding[4] and effective bond-orbital models,[5] as well as envelope function schemes with the finite-element,[6] plane-wave expansion,[7,8] and adiabatic approaches,[9,10] etc. Band structures,[6,8] interband[8] and intersubband optical transitions,[9] the exciton effect,[7,8] electron relaxation due to LO-phonon scatterings,[10] and the effect of strains[6] in V-QWR's have been investigated. In this paper, we present the calculated result of the electronic states of V-QWR's in external electric fields, which to our knowledge has not been reported in the literature. Applying electric fields to V-QWR's is the simplest way by which the system can be used to design tunable devices.

The V-QWR structure is modeled by two V-shaped interfaces $y_{1,2}=f_{1,2}(x)$ which separate the GaAs well between $Al_xGa_{1-x}As$ barrier regions, as shown in Fig. 1(a). The calculation is carried out with the theory we developed previously,[11] which overcomes the difficulty due to the complicated boundary conditions of the electron wave functions on the nonplanar interfaces of the V-QWR. In the effective-mass approximation, the eigenvalue equation and boundary conditions of the electrons are obtained by requiring the first-order difference of the following functional be equal to zero ($\delta L[\psi]=0$), with the functional $L[\psi]$ given by

$$L[\psi]=\int\left\{\frac{\hbar^2}{2m_e(\mathbf{r})}|\nabla\psi(\mathbf{r})|^2+[V(\mathbf{r})+e\mathbf{F}\cdot\mathbf{r}-E]|\psi(\mathbf{r})|^2\right\}d\mathbf{r}, \tag{1}$$

where $m_e(\mathbf{r})$ is the electron effective mass. $V(\mathbf{r})$ is the band offset between bulk GaAs and $Al_xGa_{1-x}As$, $\mathbf{F}$ is the applied electric field, and E is the electron energy to be determined.

To find an appropriate complete set of functions to expend the wave function ψ of the electron, we introduce the coordinate transformation[11]

$$\tilde{x}=x,$$

$$\tilde{y}=D\{y-[f_1(x)+f_2(x)]/2\}/[f_1(x)-f_2(x)], \tag{2}$$

$$\tilde{z}=z,$$

which transforms the V-QWR in space $\mathbf{r}$ to a quantum well (QW) with planar interfaces at $\tilde{y}_{\pm}=\pm D/2$ in space $\tilde{\mathbf{r}}$, as shown in Fig. 1(b). In space $\tilde{\mathbf{r}}$, the wave function $\tilde{\psi}(\tilde{\mathbf{r}})$ of the electron is expended with the eigenwave functions $\zeta_l(\tilde{y})$ of the corresponding QW:

$$\tilde{\psi}_n(\tilde{\mathbf{r}})=\sum_{l=1}^{L_0}\sum_{m=0}^{M_0}A_{lm}^{(n)}\eta_m(\tilde{x})\zeta_l(\tilde{y}). \tag{3}$$

The selection of the expansion functions $\eta_m(\tilde{x})$ in the $\tilde{x}$ direction depends on the profile of the interfaces of the V-QWR, which determines the effective potential introduced into the Hamiltonian of the system after the coordinate transformation. For V-QWR's fabricated at present, their interfaces are approximately parabolic, at least near the central region ($x=0$). We take $\eta_m(\tilde{x})$ as the eigenwave functions of the following harmonic oscillator:

$$-\frac{\hbar^2}{2m_{\mathrm{GaAs}}}\frac{d^2}{d\tilde{x}^2}\,\eta_m(\tilde{x})+\frac{1}{2}m_{\mathrm{GaAs}}\omega^2\tilde{x}^2\eta_m(\tilde{x})=\epsilon_m\eta_m(\tilde{x}). \tag{4}$$

The width D of the QW and angular frequency ω of the harmonic oscillator are taken as the adjustable parameters to insure the fastest convergence of the expansion in Eq. (3). Substituting $\tilde{\psi}_n(\tilde{\mathbf{r}})$ into the functional $\tilde{L}[\tilde{\psi}_n]$ in space $\tilde{\mathbf{r}}$ and setting $\partial\tilde{L}[\tilde{\psi}_n]/\partial A_{lm}^{(n)}=0$, we obtain the eigenvalue equation which determines the energy and wave function of the electron in the V-QWR.

When a constant electric field is applied to the V-QWR, strictly speaking, no bound state exists if the barrier height of the V-QWR is finite. The electrons will finally tunnel out of the V-QWR. However, the tunneling becomes negligible in the V-QWR's with wide well widths or in weak electric fields.[12] The (quasi) bound states exist in the V-QWR. To be consistent with the limitation of weak electric fields, the effect of the electric fields on the electron states of the V-QWR can be analyzed by the above perturbation method, where the

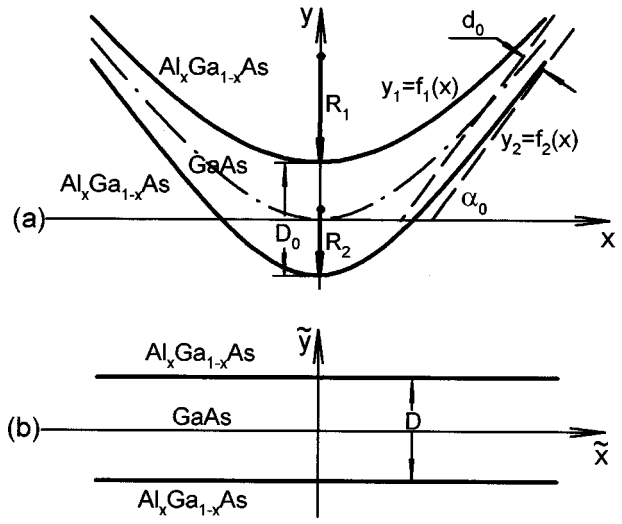

FIG. 1. (a) The GaAs/$Al_xGa_{1-x}As$ V-QWR that we considered in the original space $\mathbf{r}$, with R_1 and R_2 the curvature radii of the interfaces at $x=0$, D_0 and d_0 the distances between the interfaces at $x=0$ and $x\rightarrow\infty$, and α_0 the angle between the lower interface and the x axis. (b) The V-QWR structure in the transformed space $\tilde{\mathbf{r}}$.

applied electric field is considered as a perturbation of the Hamiltonian, while the bound states of the V-QWR are expanded with the eigenwave functions in the zero electric fields.

As a model calculation, we consider the following GaAs/$Al_xGa_{1-x}As$ V-QWR characterized by the curvature radii (R_1,R_2) of the interfaces at $x=0$, the distances $(D_0,\ d_0)$ between the interfaces at $x=0$ and $x\rightarrow\infty$, and the angle (α_0) between the lower interface and x axis [see Fig. 1(a)], with the interface profile given by

$$f_i(x)=k\sqrt{x^2+\alpha^2}-k\alpha-(-1)^i\frac{D_0}{2}+(i-1)\frac{\beta^2x^2}{\gamma^2+x^2}, \tag{5}$$

where $i=1$ and 2, and the parameters k, α, β, and γ are determined by D_0, d_0, R_1, R_2, and α_0. The accuracy of the calculation is tested by varying the number (L_0,M_0) of the expansion functions used in Eq. (3). For the V-QWR's that we considered below, rapid convergence in the electron wave function expansion is observed for $L_0=4$ and $M_0=8$.

In Fig. 2, the calculated electronic energy levels E_n ($n=0$ and 1) of the V-QWR are given as functions of (a) the vertical F_y and (b) the lateral electric field F_x. The structural parameters of the V-QWR are $D_0=20$ nm, $d_0=0$, $R_1=25$ nm, $R_2=12.5$ nm, and $\alpha_0=55°$. The electron effective mass of $Al_xGa_{1-x}As$ and the band offset between GaAs and $Al_xGa_{1-x}As$ are taken as $m_e=(0.067+0.083x)m_0$ and $V_0=748.2x$ (meV),[12] with a mole fraction of Al $x=0.32$. The intersubband transition energy $\Delta E_{0-1}=E_1-E_0$ (the dash-dotted line) of the V-QWR changes sensitively as the vertical electric field F_y changes. This is because when the electron is shifted by F_y toward the lower (upper) interface of the V-QWR [see Fig. 1(a)], the localization potential in the lateral x direction becomes stronger (weaker), which increases (decreases) the energy separation of the electron subbands.

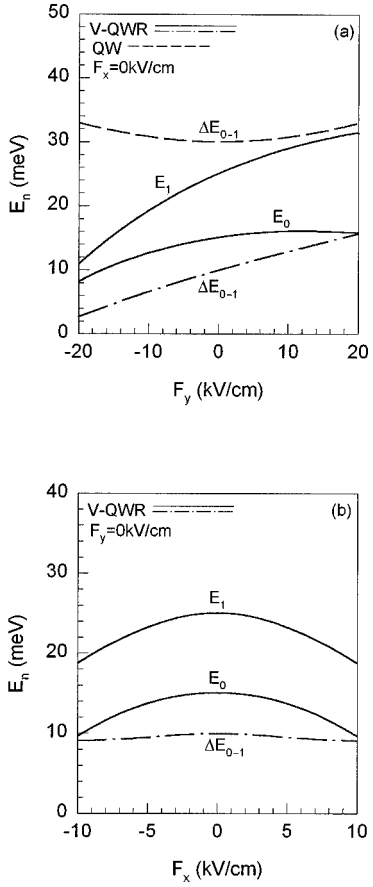

FIG. 2. The calculated electronic energy levels E_n ($n=0,1$) and intersubband transition energy ΔE_{0-1} (the dash-dotted line) of the V-QWR as functions of (a) the vertical electric field F_y and (b) the lateral electric field F_x. The structural parameters of the V-QWR are $D_0=20$ nm, $d_0=0$, $R_1=25$ nm, $R_2=12.5$ nm, and $\alpha_0=55°$. Also given in (a) is ΔE_{0-1} (the dashed line) of a GaAs/$Al_xGa_{1-x}As$ QW with a well width $D_0=20$ nm.

On the other hand, the Stark shift of ΔE_{0-1} due to the lateral electric field F_x is small, though the subband energies themselves shift quadratically as F_x changes [Fig. 2(b)]. As a comparison, in Fig. 2(a) we also plot ΔE_{0-1} (the dashed line) of a GaAs/$Al_xGa_{1-x}As$ QW with a well width $D_0=20$ nm.

In Fig. 3, we give the square of the momentum matrixes $|\mathbf{e}\cdot\mathbf{P}_{0-n}|^2$ calculated for the intersubband transitions from the lowest to higher energy levels ($n=1,2,\ \ldots$), with incident lights polarized in the direction $\mathbf{e}$. $|\mathbf{e}\cdot\mathbf{P}_{0-n}|^2$ is plotted as functions of (a) F_y and (b) F_x, as defined in Fig. 2 for the same V-QWR. The strongest intersubband transition appears between the lowest and first excited states of the V-QWR, with the incident lights polarized in x direction. The strength of the intersubband transitions varies sensitively as the electric field changes.

In Fig. 4, the calculated electron distributions $|\psi_n(x,y)|^2$ of the lowest [$n=0$ in Figs. 4(a), 4(c), 4(e), and 4(g)] and first excited states [$n=1$ in Figs. 4(b), 4(d), 4(f), and 4(h)] are plotted in space $\mathbf{r}$ for the same V-QWR as that in Fig. 2. The applied electric field is (a) and (b) $\mathbf{F}=0$, (c) and (d) $F_x=0$, $F_y=-20$ kV/cm, (e) and (f) $F_x=0$ and $F_y=20$ kV/cm, and (g) and (h) $F_x=-10$ kV/cm, $F_y=0$. The x-y axes in $|\psi_0(x,y)|^2$ [Figs. 4(a), 4(c), 4(e), and 4(g)] are turned by

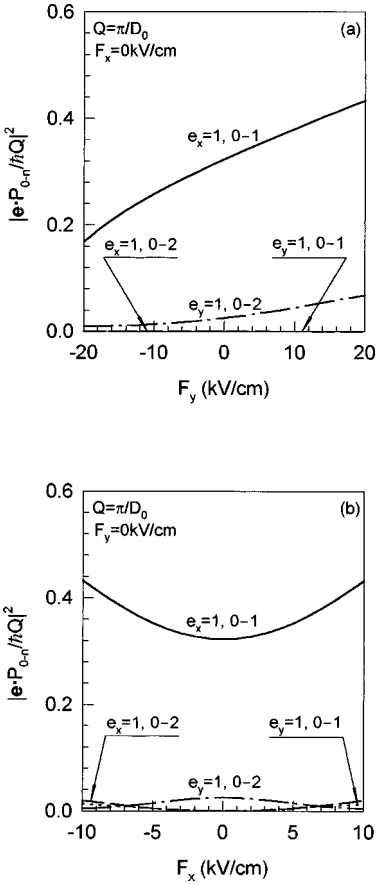

FIG. 3. The square of the momentum matrixes $|\mathbf{e}\cdot\mathbf{P}_{0-n}|^2$ calculated for the intersubband transitions from the lowest to higher energy levels ($n=1,2,\ldots$), with incident lights polarized in the direction $\mathbf{e}$. $|\mathbf{e}\cdot\mathbf{P}_{0-n}|^2$ is plotted as functions of (a) F_y and (b) F_x as defined in Fig. 2. The structural parameters of the V-QWR are the same as those in Fig. 2.

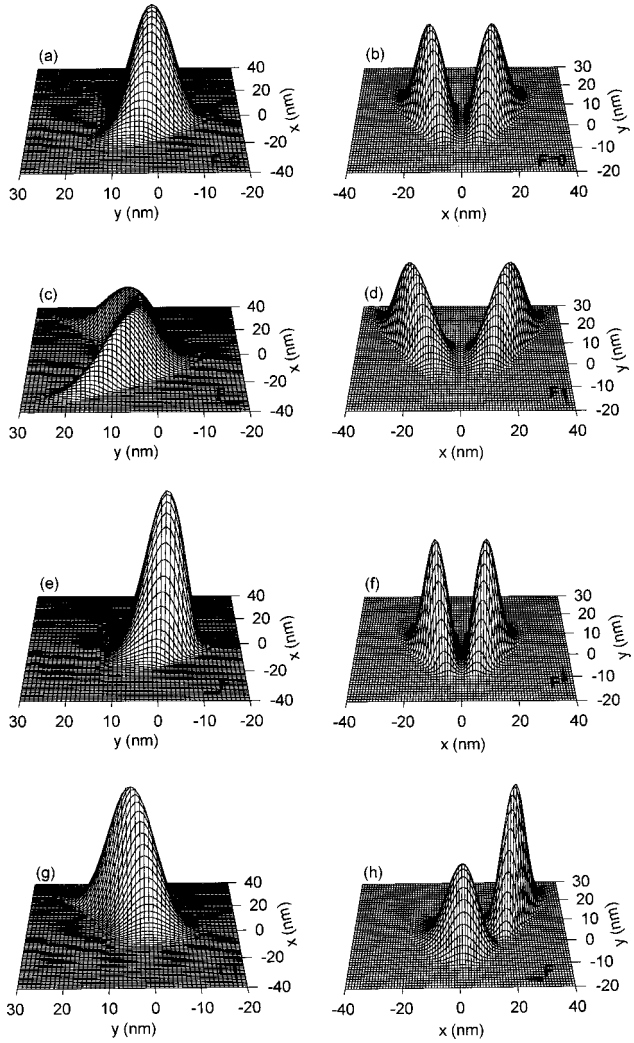

FIG. 4. The calculated electron distributions $|\psi_n(x,y)|^2$ of the lowest states [$n=0$ in (a), (c), (e), and (g)] and first excited states [$n=1$ in (b), (d), (f), and (h)] for the same V-QWR as in Fig. 2. The applied electric fields are (a) and (b) $\mathbf{F}=0$, (c) and (d) $F_x=0$ and $F_y=-20$ kV/cm, (e) and (f) $F_x=0$ and $F_y=20$ kV/cm, and (g) and (h) $F_x=-10$ kV/cm and $F_y=0$. To show the main features of the electron distributions more clearly, the x-y axes in $|\psi_0(x,y)|^2$ [(a), (c), (e), and (g)] are turned by 90° in $|\psi_1(x,y)|^2$ [(b), (d), (f), and (h)].

90° in $|\psi_1(x,y)|^2$ [Figs. 4(b), 4(d), 4(f), and 4(h)], in order to show the main features of the electron distributions more clearly. The sensitive dependence of the electron distributions on the applied electric fields results in the sensitive variation of the intersubband transition energy ΔE_{0-1} and intersubband transition strength $|\mathbf{e}\cdot\mathbf{P}_{0-n}|^2$ of the V-QWR's as we discussed above.

To summarize, the electronic states of the GaAs/Al_xGa_{1-x}As V-QWR's in applied electric fields are calculated with the theory we developed previously, which overcomes the difficulty due to the complicated boundary conditions of the electron wave functions on the nonplanar interfaces of theV-QWR's. Large Stark shifts in the intersubband transition energies and sensitive variations in the intersubband transition strengths are predicated in the V-QWR's that we considered at moderate electric fields ($|F|\leqslant 20$ kV/cm).

This work was supported by the National Natural Science Foundation of China, The Pan-Deng Program of the Chinese National Committee of Science, and the Direct Grant for Research of the Chinese University of Hong Kong under Contract No. 2060137. The author is grateful to Professor K. W. Yu for the instructive discussions on the subject, and hospitality received during his stay in the Chinese University of Hong Kong.

*Electronic address: shong@mail.sjtu.edu.cn

[1] E. Kapon, D.M. Hwang, and R. Bhat, Phys. Rev. Lett. **63**, 430 (1989).

[2] S. Tiwari, G.D. Pettit, K.R. Milkove, F. Legoues, R.J. Davis, and J.M. Woodall, Appl. Phys. Lett. **64**, 3536 (1994).

[3] A. Gustafsson, B. Dwir, F. Reinhardt, G. Biasiol, J.M. Bonard, and E. Kapon, in *Proceedings of the 9th Conference on Microscopy of Semiconductor Materials, 20–23 March, Oxford, 1995.* (IOP, Bristol, 1995), p. 375.

[4] Y. Arakawa, T. Yamauchi, and J.N. Schulman, Phys. Rev. B **43**, 4732 (1991).

[5] D.S. Citrin and Y.C. Chang, IEEE J. Quantum Electron. **29**, 97 (1993).
[6] O. Stier and D. Bimberg, Phys. Rev. B **55**, 7726 (1997).
[7] R. Rinaldi, R. Cingolani, M. Lepore, M. Ferrara, I.M. Catalano, F. Rossi, L. Rota, E. Molinari, P. Lugli, U. Marti, D. Martin, F.M. Gemoud, P. Ruterana, and F.K. Reinhart, Phys. Rev. Lett. **73**, 2899 (1994).
[8] G. Goldoni, F. Rossi, E. Molinari, and A. Fasolino, Phys. Rev. B **55**, 7110 (1997).
[9] A. Sa'ar, A. Givant, S. Calderon, O.B. Shalom, E. Kapon, A. Gustafasson, D. Oberli, and C. Caneau, Superlattices Microstruct. **19**, 217 (1996).
[10] C. Ammann, M.A. Dupertuis, U. Bockelmann, and B. Deveaud, Phys. Rev. B **55**, 2420 (1997).
[11] H. Sun, J.M. Huang, and K.W. Yu, J. Phys.: Condens. Matter **8**, 7605 (1996).
[12] G. Lengyel, K.W. Jelley, and R.W.H. Engelmann, IEEE J. Quantum Electron. **26**, 296 (1990).